Phonons and magnetic excitations in the Mott insulator $LaTiO_3$

M. N. Iliev,[1] A. P. Litvinchuk,[1] M. V. Abrashev,[2] V. N. Popov,[2] J. Cmaidalka,[1] B. Lorenz,[1] and R. L. Meng[1]
[1]*Texas Center for Superconductivity and Advanced Materials, and Department of Physics, University of Houston, Houston, Texas 77204-5002, USA*
[2]*Faculty of Physics, University of Sofia, 1164 Sofia, Bulgaria*

(Received 24 September 2003; revised manuscript received 5 March 2004; published 12 May 2004)

The polarized Raman spectra of stoichiometric $LaTiO_3$ ($T_N = 150$ K) were measured between 6 and 300 K. In contrast to earlier report on half-metallic $LaTiO_{3.02}$, neither strong background scattering nor Fano shape of the Raman lines was observed. The high-frequency phonon line at 655 cm^{-1} exhibits anomalous softening below T_N: a signature for structural rearrangement. The assignment of the Raman lines was done by comparison to the calculations of lattice dynamics and the nature of structural changes upon magnetic ordering is discussed. The broad Raman band, which appears in the antiferromagnetic phase, is assigned to two-magnon scattering. The estimated superexchange constant $J = 15.4 \pm 0.4$ meV is in excellent agreement with the result of neutron-scattering studies.

DOI: 10.1103/PhysRevB.69.172301 PACS number(s): 78.30.Hv, 63.20.Dj, 75.30.Ds, 75.50.Ee

There is still debate on the role of orbital degrees of freedom in the antiferromagnetism of $LaTiO_3$ and whether orbital ordering exists in the antiferromagnetic phase. Neutron and resonant x-ray-scattering results of Keimer *et al.*[1] have been interpreted as evidence for orbital fluctuations, consistent with orbital liquid model of Khaliullin and Maekawa.[2] It has been pointed out[1] that earlier Raman results of Reedyk *et al.*,[3] where large background and Fano shape of the phonon line near 300 cm^{-1} have been observed, may also indicate orbital fluctuations coupled to lattice vibrations. Some recent experimental results on the temperature dependence near T_N of neutron and x-ray diffraction, heat capacity, and infrared spectra,[4–6] however, provide evidence for noticeable deformation of TiO_6 octahedra and structural anomaly near the antiferromagnetic ordering, which indirectly supports the concept of orbital ordering.

The observation in the Raman spectrum of structureless background and Fano interference is not expected for *insulating* rare-earth titanates. At the same time, it is known that transport and magnetic properties of $LaTiO_3$ depend crucially on sample's stoichiometry[7–9] and, hence, dependence on stoichiometry may be expected also for the Raman spectra. Indeed, anomalous variation of phonon Raman intensities and linewidths has been reported at 50 K for $LaTiO_{3+\delta/2}$ near the metal-to-Mott-insulator transition at $0.01 < \delta < 0.04$.[10] The room-temperature dc resistivity ($\rho = 0.02\ \Omega$ cm) of the $LaTiO_3$ sample used in the Raman experiments of Reedyk *et al.*[3] is much lower than that reported for nearly stoichiometric samples [$\rho > 0.5\ \Omega$ cm (Refs. 7 and 8)] and rather corresponds to $\delta = 0.04$. Therefore, it is of definite interest to examine the Raman spectra of stoichiometric $LaTiO_3$ in a broad temperature range including Néel temperature T_N as the variation of the Raman spectra with decreasing temperature below T_N may provide additional information on the issues of Fano interference and magnetic-order-induced orbital ordering.

In this paper we present polarized temperature-dependent Raman spectra of stoichiometric $LaTiO_3$ ($T_N = 150$ K) between 6 and 300 K. At room temperature, in contrast to Ref. 3, neither strong background scattering nor Fano shape of the Raman lines is observed. The temperature shift of some Raman lines exhibits clear anomaly below T_N: a signature for structural rearrangement. We discuss the assignment of the Raman lines to definite phonon modes and the nature of structural changes. The broad Raman band, which appears in the antiferromagnetic phase, is assigned to two-magnon scattering.

$LaTiO_3$ samples were prepared using La_2O_3 (99.99%), TiO_2 (99.99%), and Ti_2O_3 (99.99%) as starting materials. La_2O_3 was heat treated at 1300 °C for 24 h and TiO_2 was dried for 24 h at 120 °C before use. Stoichiometric amounts of La_2O_3, Ti_2O_3, and TiO_2 were mixed and arc-melted under argon to form black bulk $LaTiO_3$. X-ray-diffraction pattern at room temperature revealed orthorhombic structure with lattice parameters $a = 5.61$ Å, $b = 7.91$ Å, and $c = 5.63$ Å, in agreement with earlier reports.[4,6] It is known that the magnetic transition temperature T_N is very sensitive to the oxygen content[8] and rapidly shifts to lower T if the oxygen composition exceeds the stoichiometric value of 3.[9] Therefore, the value of T_N is a precise measure of the oxygen stoichiometry in $LaTiO_3$. The weak ferromagnetism is due to the asymmetric Dzyaloshinsky-Moriya exchange interaction and can easily be picked up in dc-susceptibility measurements.

For our sample the superconducting quantum interference device magnetometry was employed to measure the magnetic transition temperature. Figure 1(a) shows the inverse susceptibility data measured at 50 Oe in the temperature range between 5 and 400 K. A sharp drop occurs at 150 K, in excellent agreement with the best available data for stoichiometric single crystals.[6] Another supportive evidence, which points to almost perfect sample stoichiometry, is the room-temperature conductivity, obtained by Kramers-Kronig transformation of near-normal reflectance. It extrapolates [Fig. 1 (b)] to the dc value of $4.5 \pm 0.5\ \Omega^{-1}\,cm^{-1}$ ($\rho = 0.22 \pm 0.03\ \Omega$ cm), which corresponds to $\delta < 0.01$.[8]

Raman spectra were collected under microscope (focus spot size 1–3 μm, $\lambda_{exc} = 514.5$ nm or 632.8 nm) from freshly cleaved or as-grown surfaces of the bulk material. The crystallographic orientation of the surface was not

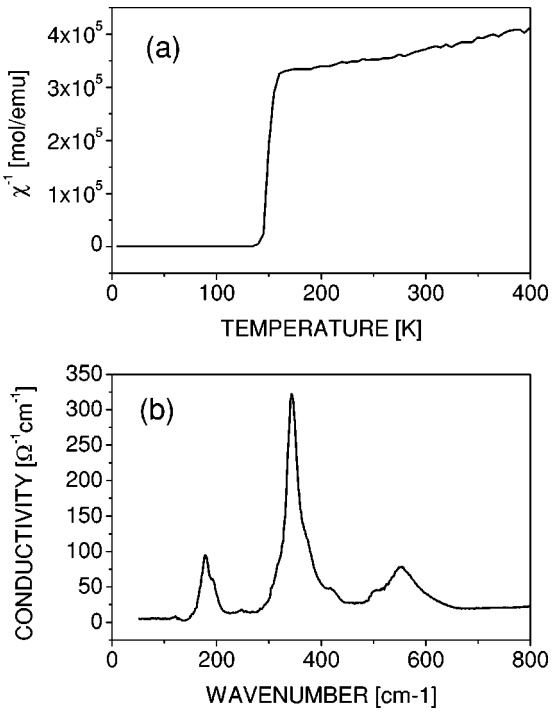

FIG. 1. (a) Inverse magnetic susceptibility of $LaTiO_3$ measured at 50 Oe as a function of temperature; (b) room-temperature conductivity, obtained from the near-normal reflectance data.

known but in most cases the spectra taken with parallel (HH) and crossed (HV) polarizations of incident and scattered radiation were totally polarized: an indication that the surface coincides with one of the main crystallographic planes (ab, bc, or ac). For temperature-dependent measurements the sample was mounted in a liquid-helium cryostat. As the Raman signals were extremely low, relatively high incident laser power (≈ 5 mW) was used, which resulted in some heating of the microprobe spot.

Figure 2 shows the polarized Raman spectra of $LaTiO_3$ as obtained at room temperature from five different spots. Three Raman lines (at 133, 252, and 296 cm^{-1}) always appear stronger in parallel (HH) scattering configuration, which indicates fully symmetric character (A_g) of the corresponding vibrations. Four other lines (at 182, 418, 465, and 655 cm^{-1}) seen in both crossed (HV) and parallel (HH) configurations are rather of ''off-diagonal'' origin (B_{1g}, B_{2g}, or B_{3g}). The phonon line positions are close to those reported by Reedyk *et al.* (see Fig. 2 in Ref. 3), but the background scattering is much weaker and the lines are narrower. The most significant difference is the observation of two clearly distinguishable symmetric lines at 252 and 296 cm^{-1} instead of one broader asymmetric band between 220 and 300 cm^{-1}. Taking into account that for $LaTiO_{3+\delta/2}$ one expects an increase of the electronic background, phonon line intensity, and phonon linewidth with increasing δ,[10] the ''Fano shaped'' band reported by Reedyk *et al.*[3] rather seems to be a complex band, consisting of two bands, broadened in doped samples by the phonon interaction with electronic continuum. Further systematic studies of phonon line shapes in $LaTiO_{3+\delta/2}$ as a function of doping might clarify this issue.

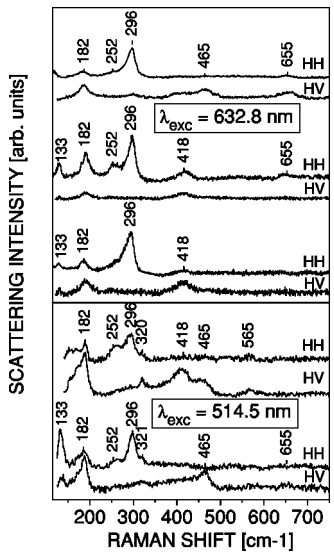

FIG. 2. Polarized Raman spectra of $LaTiO_3$ as obtained at room temperature from several different spots with 632.8 nm (upper panel) and 514.5 nm (lower panel) excitation.

The variations with temperature of the HH and HV Raman spectra are shown in Fig. 3. Upon lowering temperature some of the lines (182 cm^{-1}, 296 cm^{-1}, and 465 cm^{-1}) exhibit normal monotonous narrowing and hardening to 196, 310, and 474 cm^{-1}, respectively. The line at 252 cm^{-1} decreases in intensity and cannot clearly be detected as the nominal temperature approaches T_N. Instead, in the antiferromagnetic phase a relatively broad line arises between 250 and 300 cm^{-1}. At low temperatures two additional lines are clearly pronounced at 402 and 431 cm^{-1} in the HV spectra.

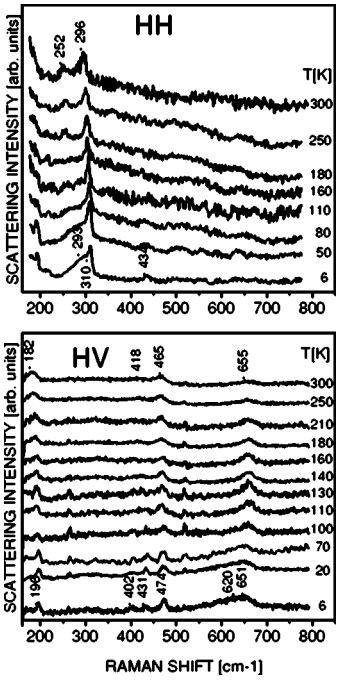

FIG. 3. Variations with temperature of the HH and HV Raman spectra of $LaTiO_3$. Due to local laser heating the actual temperature is higher than the nominal one.

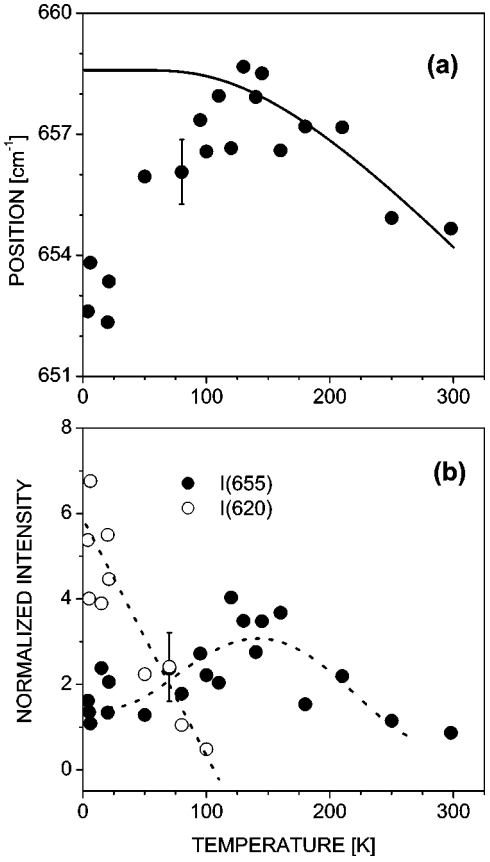

FIG. 4. Temperature dependence of the phonon line position (a) and intensities (b) of the two high-frequency HV bands near 655 cm^{-1} and 620 cm^{-1} normalized to the intensity of the 465 cm^{-1} HV line. Solid line in (a) shows the behavior expected for a standard anharmonic phonon decay and dotted lines in (b) are guide to the eye.

The line, which exhibits anomalous temperature behavior, is the one at 655 cm^{-1}. As illustrated in Fig. 4, with lowering temperature between 300 K and 130 K this mode hardens and increases in intensity. Upon further cooling, however, it moves back to lower wave numbers and merges with an arising new broadband centered at about 620 cm^{-1} (see also Fig. 5). The position of the latter band is independent of temperature within the experimental error (± 15 cm^{-1}) and its intensity increases much faster compared to intensity decrease of the 655 cm^{-1} phonon line.

In order to assign the observed Raman lines to definite phonon modes we performed lattice-dynamical calculations (LDC) using a shell model, which has been applied earlier for isostructural $YMnO_3$ and $LaMnO_3$.[11] To evaluate the effect of structural changes, identical calculations were done using the neutron-diffraction data of Cwik *et al.*[4] for atomic positions at 8 K, 155 K, and 293 K. The LDC results (Table I) show that both the predicted frequencies and shapes of the phonon modes of $LaTiO_3$ and $LaMnO_3$ are very close. The three HH lines can unambiguously be assigned to A_g modes involving mainly motions of La along z (133 cm^{-1}), in-phase rotations around y of neighboring (along y) TiO_6 octahedra (252 cm^{-1}), and O1 motions in the xz plane (295 cm^{-1}), respectively. The assignment of the rest lines is

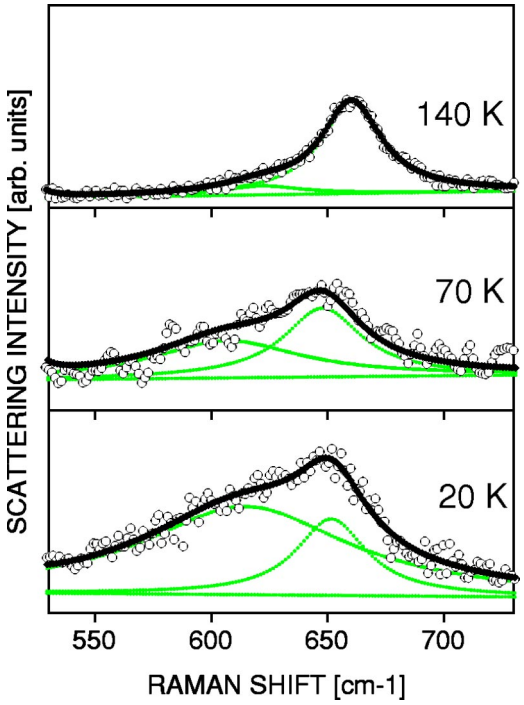

FIG. 5. Evolution of the two-magnon band upon lowering temperature. The experimental data are represented by open points.

TABLE I. Experimentally observed and calculated Raman phonon frequencies (in cm^{-1}) of $LaTiO_3$.

Raman mode	Expt. 293 K	LDC 293 K	LDC 155 K	LDC 8 K
$A_g(1)$		105.2	107.1	108.5
$A_g(2)$	133	150.9	152.1	152.9
$A_g(3)$	252	238.4	243.7	247.3
$A_g(4)$	296	294.5	295.9	297.3
$A_g(5)$		347.0	349.0	351.4
$A_g(6)$		474.1	475.6	476.7
$A_g(7)$		496.0	496.7	497.2
$B_{1g}(1)$		175.4	176.4	176.4
$B_{1g}(2)$		259.0	263.0	264.4
$B_{1g}(3)$		344.2	345.3	345.4
$B_{1g}(4)$		487.2	487.8	488.0
$B_{1g}(5)$		637.6	639.1	638.0
$B_{2g}(1)$		110.3	111.4	112.0
$B_{2g}(2)$	182	157.1	157.9	158.9
$B_{2g}(3)$		254.2	256.6	260.7
$B_{2g}(4)$	418	353.6	357.6	359.9
$B_{2g}(5)$	465	467.3	467.8	468.3
$B_{2g}(6)$		507.8	508.3	509.3
$B_{2g}(7)$	655	640.2	640.3	640.7
$B_{3g}(1)$		147.5	148.1	148.5
$B_{3g}(2)$		339.5	339.8	339.7
$B_{3g}(3)$		472.4	472.8	473.1
$B_{3g}(4)$		500.0	502.1	501.2
$B_{3g}(5)$		651.8	652.3	651.9

less straightforward as to each of them one can juxtapose B_{1g}, B_{2g}, or B_{3g} mode of close predicted frequency. Whatever is the choice, the line at 182 cm^{-1} corresponds to a mode involving mainly motions of La and the line at 655 cm^{-1} to in-phase (B_{2g}) or out-of-phase (B_{1g},B_{3g}) stretching of TiO_6 octahedra.

The comparison of frequencies calculated using structural data at 8 K, 155 K, and 293 K provides evidence that the softening of the 655 cm^{-1} mode below T_N is related, at least partly, to the structural changes induced by magnetic ordering.[4] These changes include elongation of TiO_6 octahedra along *c* (in *Pnma* notations) by 0.2%, shrinking along *a* by 0.3%, and an anomalous shortening of the Ti-O1 distance near T_N. Indeed, the LDC results predict hardening of all Raman modes except for the B_{1g}, B_{2g}, and B_{3g} modes near 650 cm^{-1}. The latter modes have maximum wave number at 155 K and then either soften by ~ 1 cm^{-1} (B_{1g},B_{3g}) or remain unchanged (B_{2g}) at 8 K. Interestingly, similar softening below T_N has also been observed for the corresponding B_{2g} mode in isostructural $LaMnO_3$ (Refs. 12–14) and interpreted by Granado *et al.*[13] in terms of spin-phonon coupling caused by phonon modulation of the superexchange integral. Another result that follows from the comparison of LDC data of $LaTiO_3$ at different temperatures is that the HH line at 252 cm^{-1} at 300 K and the broadband at $\approx$290 cm^{-1} at 6 K most likely correspond to the same ''soft'' mode. It is worth noting that all predicted temperature shifts due to structural changes are by a factor of 3 smaller than the experimentally observed ones. The reason for this discrepancy is not clear.

The broad structure between 570 and 650 cm^{-1} appears only below T_N and strongly increases with lowering temperature (see Fig. 5) thus identifying itself as related to magnetic excitations. The magnon dispersion curve for $LaTiO_3$ along the pseudocubic [111] direction was measured by Keimer *et al.*[1] and fitted by the expression $\hbar\omega = zSJ\sqrt{1.005-\gamma^2}$, where $\hbar\omega$ is the magnon energy, $z=6$ is the coordination number, $S=1/2$ is the Ti spin, $J=15.5 \pm 1.0$ meV is the nearest-neighbor superexchange energy, and $\gamma=\frac{1}{3}[\cos(q_x a)+\cos(q_y a)+\cos(q_z a)]$. The zone-center magnons ($\gamma=1$,$\hbar\omega=3.3$ meV) are far below our range of measurement and only second-order magnetic scattering is expected. The intensity of the two-magnon scattering is determined by the magnitude of the two-magnon density of states, which has maximum at the zone boundary, and by the interaction of the two magnons created in the scattering process. The latter interaction results in creation of a ''bound state,'' which decreases the two-magnon energy by *J* compared to the sum of individual magnon energies at the boundary $2zSJ$.[15,16] Therefore, the maximum of two-magnon scattering for $LaTiO_3$ is expected at $\hbar\omega_{2M}=2zSJ-J=5J$. The position of the broad line in the spectra is 620 ± 15 cm^{-1} (76.9 ± 2.0 meV) yields $J=15.4\pm 0.4$ meV, in excellent agreement with the results of neutron-scattering experiments.[1]

This work was supported in part by the state of Texas through the Texas Center for Superconductivity and Advanced Materials.

[1] B. Keimer, D. Casa, A. Ivanov, J.W. Lynn, M.v. Zimmermann, J.P. Hill, D. Gibbs, Y. Taguchi, and Y. Tokura, Phys. Rev. Lett. **85**, 3946 (2000).
[2] G. Khaliullin and S. Maekawa, Phys. Rev. Lett. **85**, 3950 (2000).
[3] M. Reedyk, D.A. Crandles, M. Cardona, J.D. Garrett, and J.E. Greedan, Phys. Rev. B **55**, 1442 (1997).
[4] M. Cwik, T. Lorenz, J. Baier, R. Müller, G. André, F. Bourée, F. Lichtenberg, A. Freimuth, E. Müller-Hartmann, and M. Braden, Phys. Rev. B **68**, 060401 (2003).
[5] J. Hemberger, H.-A. Krug von Nidda, V. Fritsch, J. Deisenhofer, S. Lobina, T. Rudolf, P. Lunkenheimer, F. Lichtenberg, A. Loidl, D. Bruns, and B. Büchner, Phys. Rev. Lett. **91**, 066403 (2003).
[6] V. Fritsch, J. Hemberger, M.V. Eremin, H.-A. Krug von Nidda, F. Lichtenberg, R. Wehn, and A. Loidl, Phys. Rev. B **65**, 212405 (2002).
[7] Y. Okada, T. Arima, Y. Tokura, C. Murayama, and N. Mori, Phys. Rev. B **48**, 9677 (1993).
[8] Y. Taguchi, T. Okuda, M. Ohashi, C. Murayama, N. Mori, Y. Iye, and Y. Tokura, Phys. Rev. B **59**, 7917 (1999).
[9] G.I. Meijer, W. Henggeler, J. Brown, O.-S. Becker, J.G. Bednorz, C. Rossel, and P. Wachter, Phys. Rev. B **59**, 11 832 (1999).
[10] T. Katsufuji and Y. Tokura, Phys. Rev. B **50**, 2704 (1994).
[11] M.N. Iliev, M.V. Abrashev, H.-G. Lee, V.N. Popov, Y.Y. Sun, C. Thomsen, R.L. Meng, and C.W. Chu, Phys. Rev. B **57**, 2872 (1998).
[12] V.B. Podobedov, A. Weber, D.B. Romero, J.P. Rice, and H.D. Drew, Phys. Rev. B **58**, 43 (1998).
[13] E. Granado, A. Garcia, J.A. Sanjurjo, C. Rettori, I. Torriani, F. Prado, R.D. Sanchez, A. Caneiro, and S.B. Oseroff, Phys. Rev. B **60**, 11 879 (1999).
[14] M.N. Iliev and M.V. Abrashev, J. Raman Spectrosc. **32**, 805 (2001).
[15] R.J. Elliot, M.F. Thorpe, G.F. Imbush, R. Loudon, and J.B. Parkinson, Phys. Rev. Lett. **21**, 147 (1968).
[16] W. Hayes and R. Loudon, *Scattering of Light by Crystals* (Wiley, New York, 1978).